Dispersions of pyrogenic alumina in pentylcyanobiphenyl studied by deuteron NMR

C. T. Yim*

Department of Chemistry, Dawson College, 3040 Sherbrooke Street West, Westmount, Québec, Canada H3Z 1A4
and Department of Chemistry, McGill University, 801 Sherbrooke Street West, Montréal, Québec, Canada H3A 2K6

(Received 5 March 2009; published 10 September 2009)

Dispersions of hydrophilic (Aeroxide Alu C) and hydrophobic (Aeroxide Alu C 805) pyrogenic alumina (Al_2O_3) in liquid crystal 4′-n-pentyl-4-cyanobiphenyl (5CB) were investigated with deuteron nuclear magnetic resonance. The disorder effects of Al_2O_3 particles on the orientational order of liquid-crystal media and on the field-induced director configuration were studied as a function of alumina density in samples prepared by zero-field cooling and in-field cooling procedures. The order parameters and their variation with alumina density suggest a stronger disordering effect from the nonpolar surface of Alu C 805 particles. For dispersions of hydrophobic Alu C 805 experiments involving in-field cooling from the isotropic phase indicate that the director of "disordered" domains can be aligned, though not perfectly, by the field-aided annealing process. But the same in-field cooling procedure has shown rather limited alignment effects for hydrophilic Alu C/5CB samples. The more robust network of hydrophilic gel possibly coupled with weak liquid-crystal-network interactions could be responsible for the observed behavior. Spectra recorded during in-field cooling and within the isotropic-nematic coexistence region reveal the augmentation of the disorder strength during the transition and illustrate the effect of field-aided annealing. The stability of the aligned states as revealed by deuteron NMR is described. The results are discussed in comparison with previous studies of aerosil dispersions in alkylcyanobiphenyl.

DOI: 10.1103/PhysRevE.80.031704 PACS number(s): 61.30.Gd, 61.30.Pq

I. INTRODUCTION

Liquid-crystal (LC) composites, particularly those composed of dispersed organic and inorganic nanoparticles in liquid-crystal hosts, have received considerable attention [1]. Systems containing nanosized pyrogenic (fumed) oxide particles, such as aerosils from Degussa (now Evonik), can exhibit the so-called "memory effect" [2–4], where the external field-induced LC orientation remains stable after removal of the field. Recently, the memory of applied fields shown by LC dispersions of pyrogenic oxides has been utilized to construct simple bistable displays with low power consumption [5]. In mixtures with aerosil, the LC molecules are confined within a relatively weak gel network formed by aerosil particles via hydrogen bonds involving the surface hydroxyl groups. Interactions with the surface of randomly dispersed particles disturb the orientational order causing elastic strains on the LC directors. Within a certain range of aerosil densities, the network could have a responsive structure, i.e., it would rearrange to relax the local elastic stress. It has been suggested that, in response to the external field, the restructuring of the aerosil network and adoption of an anisotropic configuration lead to the stabilization of the field-induced alignment and thus the observed memory effect. However, Bellini *et al.* [6] showed by experimental and Monte Carlo simulation studies that memory effects are present in nematics with quenched disorder imposed by a host matrix that does not allow reorganization. They argued that pinning of the defect lines leads to the memory effect, although they recognize the possibility of local reordering of the solid network in LC-aerosil dispersions, particularly, during in-field cooling (IFC) through the isotropic to nematic phase transition. Since our experimental method requires the presence of a strong external field, anisotropic restructuring of the gel network is probably responsible for the "memory" effects observed in our systems [7].

Dispersing nanoparticles in a LC disturbs the long-range order of the mesophase and can be viewed as introducing a random disorder field into the medium. The effects of random disorder on physical systems are of fundamental interest and have been the focus of many theoretical and experimental studies. Over the past decade, dispersions of hydrophobic and hydrophilic aerosil particles in alkylcyanobiphenyl (nCB) LC solvents have become experimental model systems for examining the effects of partially and fully quenched random disorders on LC phase transition behaviors. The disorder effects and the LC-network interactions have been assessed systematically by varying the amount of dispersed aerosil [8]. The effect of both the hydrophilic and the hydrophobic aerosils on phase transitions of 8CB (4′-n-octyl-4-cyanobiphenyl) has been the subject of many studies and the results were summarized in a recent review [9]. Aerosil dispersions in 8CB have also been investigated with deuteron NMR and with ESR (electron spin resonance) as well [10,11]. Recently, the results of a deuteron NMR study of dispersions of hydrophilic and hydrophobic aerosils in a Schiff-base-type LC, EBBA [N-(4-ethoxybenzylidene)-4-n-butylaniline], have been published [12]. In comparison, relatively little work has been done on other composites composed of nanoparticles of different chemical compositions. Studies of systems with distinct different characters could provide insights on the nature of LC-particle interactions and could enable us to isolate material specific effects.

The "aerosil" process, i.e., high-temperature hydrolysis of the corresponding chlorides, has been employed by Degussa to produce nanosized metal oxides: mainly, aluminum oxide,

*c.yim@mcgill.ca

titanium dioxide, and zirconium oxide [13]. Similar to aerosils, pyrogenic metal oxide particles have no internal surface and hydroxyl groups are present on the particle surface. Likewise, their primary particles form irregular and branched aggregates and agglomerates. The particles of all three pyrogenic metal oxides have well-defined structures, which can be assigned to known crystalline forms. In comparison, aerosil fumed silica from Degussa is x-ray amorphous, as shown by the absence of defined diffraction rings or lines in the x-ray photograph. Because of their higher density, dispersions of metal oxide in polar or nonpolar media could show reduced stability with respect to sedimentation.

This work deals with dispersions of Degussa alumina (Al_2O_3) particles in liquid-crystal 4′-n-pentyl-4-cyanobiphenyl (5CB). Systems containing either the hydrophilic (Aeroxide Alu C) or the surface modified hydrophobic Al_2O_3 (Aeroxide Alu C 805) in deuterated 5CB were systematically investigated by deuteron NMR (DNMR). The Alu C particles are small Al_2O_3 spheres with an average diameter of 13 nm and a specific surface area of 100 ± 15 m^2/g [13]. The surface hydroxyl groups of hydrophilic alumina show more basic character than those of hydrophilic aerosil. It has been shown by infrared spectroscopy that the surface of Alu C is covered with several types of -OH groups that have somewhat different *basic* properties [13]. Thus, pyrogenic alumina Alu C possesses a basic and chemically more complex surface. Nevertheless, like aerosils, when dispersed in organic media the surface hydroxyl groups tend to form hydrogen bonds leading to the formation of a thixotropic gel network, which can be broken down or modified by mechanical forces or under shearing. It has been shown that dispersions of pyrogenic alumina in nCB show similar memory effects [5]. The liquid crystal 5CB has a highly polar head group and a dipole moment of ~6 D. It is known that in bulk, the 5CB molecules form "pairs" with overlapping aromatic cores and with their head groups pointing antiparallel to each other. We will draw on reported behaviors and properties of well-studied aerosil/nCB dispersions to discuss, to rationalize, and to interpret our results. This approach is adopted to elucidate the similarities as well as the differences between aerosil and alumina gels.

Deuteron NMR, dominated by the coupling between the electric quadrupole moment of the deuteron and the local electric field gradient, has been widely used for the study of the orientational order of liquid crystals. The molecules in a nematic phase are partially aligned with respect to the domain director. As a consequence, the DNMR spectrum of deuterons located on specific C–D bonds contains a quadrupolar splitting given by

$$\Delta\nu = (3/8)qS(3\cos^2\theta - 1)\langle 3\cos^2\beta - 1\rangle. \quad (1)$$

Here q is the deuterium quadrupolar coupling constant, usually taken to be 170 kHz for an aliphatic C–D bond. S is the molecular orientational order parameter and θ is the angle between the magnetic field B and the domain director. β is the angle between the C–D bond and the long molecular axis and the angular brackets $\langle\cdots\rangle$ indicate averaging over the conformational changes in the molecule. For the LC used in this study, 5CB-αd_2, which is deuterated at the first methylene group of the hydrocarbon chain, and with the para-axis of the aromatic core taken as the long molecular axis, one obtains $\beta = 109.5°$ and $\langle 3\cos^2\beta - 1\rangle = -0.666$. In writing Eq. (1), the electric field gradient tensor is assumed to be cylindrically symmetric about the C–D bond.

In bulk, LC directors are uniformly aligned along the magnetic field and $\theta = 0$, resulting a simple doublet spectrum. With composites, the LC molecules are confined in the network voids and the quantities in Eq. (1), S and θ, and, therefore, $\Delta\nu$ may show a positional dependence. Thus, depending on the dispersion concentration, the observed spectrum can vary from a bulklike doublet to a Pake pattern, reflecting a random isotropic orientation of the domain directors due to the dominant surface effect.

It is of interest to note that in many deuteron NMR studies of liquid crystals in complex geometries, Anopore membranes with the same chemical composition Al_2O_3, have been used as the confining matrix [14,15]. The Anopore membranes composed of amorphous alumina are produced by anodic oxidation of aluminum metal in strong acid media [16]. The membranes have cylindrical channels of almost uniform diameter (for example, 20, 100, or 200 nm) oriented perpendicular to the membrane surface and penetrating straight through it thickness. The Anopore membranes provide a restrictive environment with well-defined geometry, which is most suitable for studying interfacial LC-substrate interactions.

II. EXPERIMENT

Hydrophilic and hydrophobic pyrogenic alumina (Aeroxide Alu C and Aeroxide Alu C 805) were obtained from Degussa. Hydrophobic Alu C 805 is produced from Alu C by surface treatment with trimethoxyoctylsilane. They have a specific surface area of 100 ± 15 m^2/g and an average primary particle size of 13 nm [13]. The liquid-crystal 5CB, deuterated at the first methylene group of the hydrocarbon chain, was synthesized following the procedure described in the literature [17]. The product was further purified by vacuum distillation. The measured nematic to isotropic transition temperature is 36.0 °C.

The alumina/5CB samples were prepared using the solvent method [18]. The alumina was dried at 110 °C overnight. For each sample, the required amount of alumina was mixed with several milliliters of acetone and the mixture was homogenized with an ultrasonic probe (Cole-Parmer 25 kHz ultrasonic processor, model 4180) for 30 min at high power setting. After the proper amount of 5CB had been added to the homogenized mixture, the solvent acetone was slowly evaporated under reduced pressure with stirring at a temperature of ~43 °C. Finally, to ensure complete evaporation of the solvent, the sample was placed under high vacuum of 0.01 mm Hg for 5 h at ~60 °C. The sample was then cooled down to room temperature, i.e., to nematic phase [zero-field cooling (ZFC), see discussion below], and stored at 30 °C in an incubator before and between DNMR experiments.

Dispersions ranging from alumina density $\rho_s = 0.05$ to $\rho_s = 0.40$ g/cm^3 were prepared. A summary of parameters that characterize the alumina/5CB dispersions is given in Table I.

TABLE I. Characteristics of alumina dispersions in 5CB.

Alumina	ρ_s (g/cm^3)	l_0 (nm)	ϕ	p (%)
Alu C	0.051	392	0.984	1.0
	0.10	200	0.970	2.0
	0.15	133	0.955	3.0
	0.20	100	0.941	4.0
	0.25	80	0.928	5.0
Alu C 805	0.050	400	0.985	1.0
	0.096	208	0.971	1.9
	0.16	125	0.952	3.2
	0.24	83	0.930	4.8
	0.30	67	0.914	6.0
	0.32	63	0.909	6.4
	0.38	53	0.894	7.6

These parameters have been used to characterize confined LC systems [8,10,19] and their symbols are defined as ρ_s =g of Al_2O_3 per cm^3 of 5CB is the alumina density in the dispersion; $l_0=2/(a\rho_s)$, with the specific surface area a =100 m^2/g, is the average void size in the gel network; ϕ is the volume fraction of the void in the gel and $p=l_b a\rho_s$ is the percentage of 5CB molecules in a boundary layer anchored by the Al_2O_3 surface [8]. In calculating these parameters, we assume that the density of solid alumina is 3.2 g/cm^3 and the thickness of the boundary layer (l_b) is 2 nm. The magnitudes of the three parameters l_0, ϕ, and p presented in Table I are comparable to those reported for aerosil/8CB dispersions with much lower dispersion densities [8,10], ranging from ρ_s=0.012 to ρ_s=0.090 g/cm^3, reflecting a smaller specific surface area of the large alumina particles. In LC gels, the disordering perturbations are introduced via interactions with the surface of the embedded solid structure and the disordering strength is expected to increase with the surface area per unit volume of LC. In terms of the parameters defined above, the quantity $a\rho_s(=2/l_0)$ specifies the surface area per cm^3 of LC. We argue that in discussions of disordering character of aerosil and alumina gels, dispersions with comparable surface areas per cm^3 of LC or with comparable l_0 values should be examined and compared [9]. DNMR spectra of aerosil/8CB dispersions with dispersion density in the range of ρ_s=0.01–0.10 g/cm^3 exhibit substantial field ordering effects [10]. If aerosil and alumina gels are structurally similar comparable field effects could be expected.

The deuterium NMR spectra were acquired with a solid echo sequence using a Chemagnetics CMX-300 spectrometer operating at 45.99 MHz in a magnetic field of 7.04 T. The $(\pi/2)$ pulse width was 2 μs and the acquisition recycle time was 0.2 s.

III. RESULTS AND DISCUSSION

Nematic samples can be prepared by two different procedures: the ZFC and the IFC procedures. In the ZFC procedure, the sample is cooled down from the isotropic phase with no external field applied, while in the IFC procedure, the cooling process and the isotropic to nematic ($I \rightarrow N$) phase transition occur in the presence of an applied external field. As shown by investigations of similar systems, the corresponding ZFC and IFC samples could show quite different spectra. In most cases, the IFC procedure leads to "well-aligned" spectra. Since the last step in our sample preparation procedure involves the cooling from isotropic to nematic phase outside the magnetic field, our samples as prepared are ZFC samples.

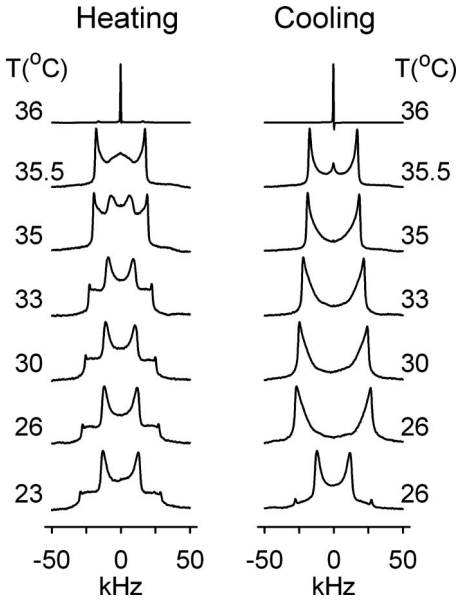

FIG. 1. Spectra of sample Alu C 805/5CB of ρ_s=3.0 g/cm^3; ZFC (left, heating) and IFC (right, cooling). The last right column spectrum was recorded after changing the sample orientation in the magnetic field by 90°.

Each prepared ZFC sample was introduced into the spectrometer probe at room temperature and subject to a heating and cooling cycle with simultaneous spectrum recording as described below. First, the spectra of the ZFC sample were recorded with increasing temperature until an isotropic spectrum was observed. The sample was then kept at ~41 °C, approximately 5 °C above the phase-transition temperature, for at least 30 min [20,21]. It was then slowly cooled down to 26 °C with a particularly slower rate of less than 0.2 °C/min through the phase-transition region. Since the $I \rightarrow N$ phase transition happened in the magnetic field of the spectrometer, the corresponding IFC nematic sample was generated. During the cooling process, the IFC spectra were recorded at selected temperatures. Finally, an additional spectrum was recorded at 26 °C after rotating the IFC sample by 90° with respect to the field direction. Examples of such ZFC and IFC spectra are shown in the left column and right column of Fig. 1, respectively, for Alu C 805/5CB dispersion of ρ_s=3.0 g/cm^3.

A. Zero-field cooling spectra

All dispersions are visibly homogeneous above their nematic to isotropic transition temperature and have a whitish

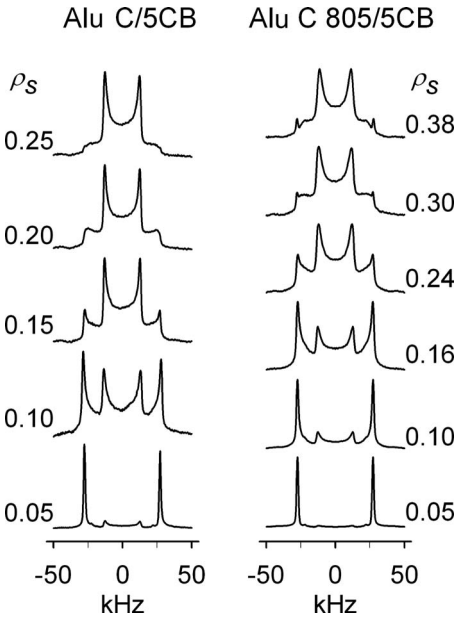

FIG. 2. Spectra at 26 °C of ZFC samples of different alumina densities ρ_s (g/cm^3): Alu C/5CB (left) and Alu C 805/5CB (right). Note the relatively sharp absorption lines at the edges of some of the powder patterns.

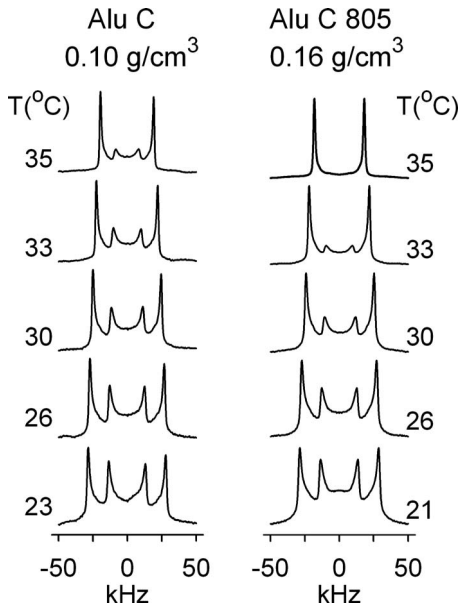

FIG. 3. Spectra of ZFC samples of Alu C/5CB ρ_s =0.10 g/cm^3 (left) and Alu C 805/5CB ρ_s=0.16 g/cm^3 (right), showing the increase in relative intensity of the narrow doublet with increasing temperature.

gel-like but opaque appearance. No phase separation was observed during the duration of the investigation. The spectra recorded at 26 °C of ZFC samples of varying alumina densities are shown in Fig. 2. Most spectra show a broad central powder pattern (i.e., Pake pattern with or without distortion) superimposed on a relatively sharp doublet usually observed for uniformly aligned bulk nematic samples. The presence of a sharp doublet in the spectra of almost all the samples studied indicates a wide distribution of void sizes and/or linkage strength in the network and LC in some voids can be easily aligned by the magnetic field. For a given type of aluminum oxide, the relative intensity of the powder pattern increases with the density ρ_s. The observed powder pattern illustrates the disordering effects of the networking Al_2O_3 particles on the enclosed LC domains.

The surface of the dispersed particles competes with the magnetic field of the spectrometer to align the domain directors. To express the relative strength of the field effect, one utilizes the parameter ξ_M, the magnetic coherence length in an external field, describing how far the surface-imposed order penetrates into the interior of a sample. In a magnetic field B, ξ_M is given by [22]

$$\xi_M = \sqrt{\frac{\mu_0 K}{\Delta\chi B^2}}, \tag{2}$$

where K is the average elastic constant and $\Delta\chi$ is the anisotropy of the volume magnetic susceptibility of the LC. Thus, for nematics located within a void of "radius" $(l_0/2) < \xi_M$, the effect of magnetic field is negligible. Field is expected to exert some effect on the alignment of domain directors in voids with $l_0/2 \approx \xi_M$. Finally, with a further increase in void sizes, a field-induced transition to the fully "aligned" state is usually observed. For example, it has been demonstrated that for spherical droplets of liquid-crystal E7 embedded in an epoxy polymer matrix, the field-induced transition to the aligned state occurs at $(d_0/2) \approx 4\xi_M$, where d_0 is the diameter of the droplet [23,24]. Based on the reported values of K [25] and $\Delta\chi$ [26–28], the magnetic coherence length of 5CB in a magnetic field B=7.04 T can be estimated. Their values decrease with temperature and are 0.34 μm and 0.27 μm at 23 °C and 34 °C, respectively. As discussed above, there is a wide distribution of void sizes in alumina gels. With decreasing ξ_M, the domain directors in smaller voids become affected by the field, leading to an increase in the relative intensity of the narrow doublet at higher temperatures, which are easily noticeable in most ZFC spectra. The spectra of two ZFC samples, Alu C/5CB of ρ_s=0.10 g/cm^3 and Alu C 805/5CB of ρ_s=0.16 g/cm^3, shown in the left and right columns of Fig. 3, respectively, exhibit a particularly strong temperature dependence, and at ~35 °C almost all the domains are aligned by the magnetic field. The average void sizes l_0 for these two systems (see Table I) are 0.20 and 0.13 μm, respectively, which are smaller than the magnetic coherence length ξ_M, 0.27 μm or 0.34 μm. In contrast to expectations, strong magnetic field ordering effects were observed even when the average $(l_0/2) < \xi_M$. Stronger than expected ordering effects on nematic directors have also been reported for aerosil dispersions in 8CB and have been interpreted as a consequence of the interconnected nature of gel voids [10]. In interconnected voids, the director configurations of neighboring LC domains are correlated and the correlation of nematic order could extend over a distance greatly exceeding the confining or void size. If we assume that full alignment of domain directors is to occur when $(d_0/2) \approx 4\xi_M$ (d_0 is the domain size), our ZFC spectra suggest a domain size (or the correlation length of the nematic order) of 2.2 μm. Thus, for considering magnetic field ordering effects on our disper-

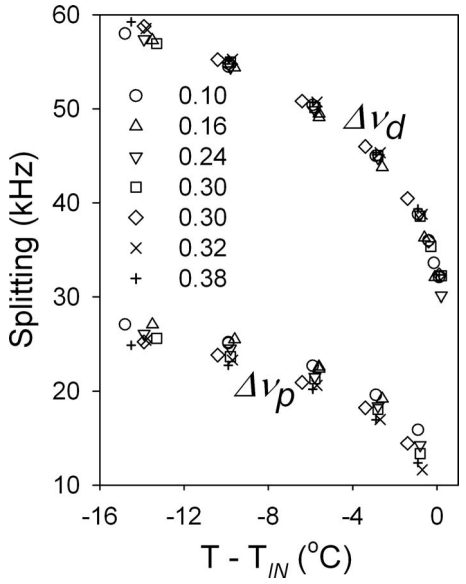

FIG. 4. Temperature dependences of the narrow doublet splitting $\Delta\nu_d$ and of the Pake pattern splitting $\Delta\nu_p$ for ZFC samples of Alu C 805/5CB. T_{IN} is the isotropic to nematic phase-transition temperature of the dispersion. Legend labels are ρ_s values in g/cm^3.

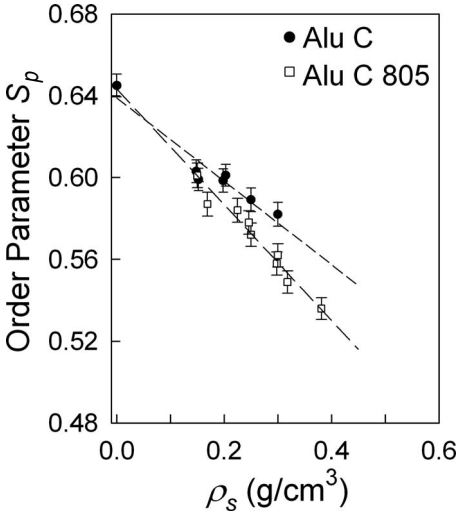

FIG. 5. The dependence on alumina density of orientational order parameter S_p for Alu C/5CB and Alu C 805/5CB dispersions at 10 °C below T_{IN}. The dash lines are drawn as guides for the eyes.

sions, it is reasonable to assume "effective" domain sizes of $\sim 10 l_0$ or greater. Almost identical values have been suggested for assessing field effects on aerosil dispersions [10]. These results illustrate the structural similarities between aerosil and pyrogenic alumina gels.

The temperature dependences of the doublet splitting $\Delta\nu_d$ and of the Pake powder pattern splitting $\Delta\nu_p$ are plotted in Fig. 4 for ZFC samples of Alu C 805/5CB. At a given $T-T_{IN}$, where T_{IN} is the isotropic to nematic phase transition temperature of the dispersion [29], $\Delta\nu_p$ decreases with increasing dispersion density, while $\Delta\nu_d$ remains almost unchanged. Similar plots can be constructed for ZFC samples of Alu C/5CB, except that $\Delta\nu_p$ values show weaker density dependence. The splitting $\Delta\nu_p$ is the frequency separation between $\pi/2$ singularities of the Pake pattern and with a uniaxial orientational order, it should equal to one half of the doublet splitting $\Delta\nu_d$ if their respective domains have the same scalar orientational order parameter S. However, for all the dispersions of Alu C/5CB or Alu C 805/5CB studied, $\Delta\nu_p$ is significantly smaller than $(\frac{1}{2})\ \Delta\nu_d$. We have noticed that several powder patterns show distorted shapes, such as patterns with more intense shoulders (Fig. 2, right column, second spectrum from the top) or with shoulders sloping toward the center (Fig. 2, left or right column, third spectrum from the top). With the help of spectrum simulation, it could be argued that small to medium distortions observed in our powder pattern spectra do not affect the splitting $\Delta\nu_p$, and the variations of $\Delta\nu_p$ values can be attributed to the change in the average orientational order parameter of the powder pattern S_p. Thus, for extracting the average S_p from the experimental $\Delta\nu_p$, just set $\theta=\pi/2$ and $\langle 3\cos^2\beta-1\rangle=-0.666$ in Eq. (1). The derived average order parameters S_p at $T-T_{IN}=-10$ °C are plotted as a function of alumina density for the two systems Alu C/5CB and Alu C 805/5CB (Fig. 5). It should be emphasized that the plotted S_p is not the average order parameter of *all* domains in a given sample but the average of the domains in smaller voids, where their orientations are not significantly altered by the applied magnetic field. Therefore in Fig. 5, we have only included data from those spectra whose central broad pattern makes a substantial intensity contribution, 80% or more, to the total observed intensity. The order parameter S_p decreases with increasing density, reflecting a greater surface effect in smaller void spaces. Of the two systems studied Alu C/5CB and Alu C 805/5CB, the latter exhibits a steeper decrease of S with alumina density, a fact that could be interpreted as indicating a stronger disordering effect from the nonpolar surface of Alu C 805 particles. At first glance, these findings seem in contrast with the expectation. The hydroxyl groups covering the Alu C particles are assumed to interact with cyano head groups of 5CB via hydrogen bonding, which is considerably stronger than the normal intermolecular forces or hydrophobic interactions. We notice the more basic character of Alu C surface that could weaken the hydrogen bonds with the cyano group: a proton or hydrogen acceptor [30]. Various studies have demonstrated that molecular ordering at a LC-substrate surface could be significantly different from that in the LC bulk and the interactions among LC molecules could affect surface orientation and surface interactions [31]. For example, a monolayer of 5CB deposited on an alumina surface of Anopore membranes has been shown to orient with the polar cyano head groups facing the substrate and with a tilt angle of $\sim 60°$ from the surface normal [32], while in the totally 5CB filled Anopore cylindrical channels of diameter 0.2 μm, the director configuration is parallel axial [15,32], an energetically favorable configuration with a weak surface effect. On the other hand, in surface modified hydrophobic Anopore channels, a planar polar director configuration was observed suggesting a homeotropic anchoring compatible with a more substantial surface effect. In addition, on a hydrophilic substrate such as Alu C, anchoring of the polar cyano head groups at the surface leads to the loss of the inversion symmetry of the bulk nematic phase. On substrates

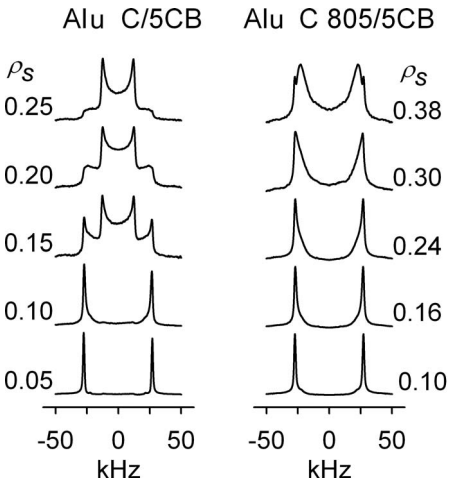

FIG. 6. Spectra at 26 °C of IFC samples of different alumina densities ρ_s (g/cm^3): Alu C/5CB (left) and Alu C 805/5CB (right).

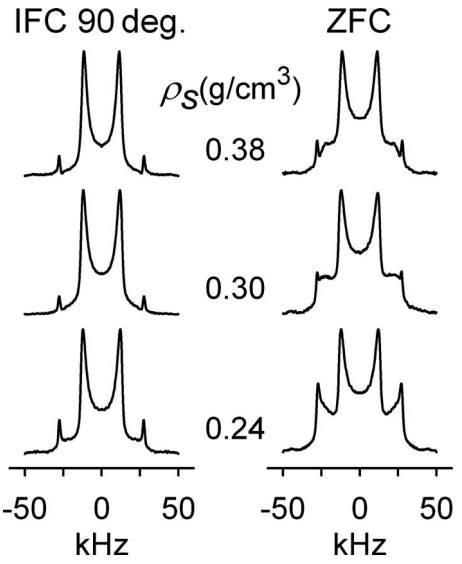

FIG. 7. IFC spectra of several Alu C 805/5CB samples at 26 °C at an orientation of 90° with respect to the magnetic field. For comparison, the corresponding spectra of ZFC samples are shown in the right column. Note the relatively sharp absorption lines at the edges of the powder pattern.

with a hydrophobic surface, the substrate-molecular interactions could orient the molecules with their alkyl chains in contact with the treated surface. Thus, the cyanobiphenyl molecules can orient and follow their natural tendency to form "pairs" and no polar order appears. The interplay of various forces and factors leading to a particular surface-effected bulk alignment and determining the disordering strength via the first LC monolayer deposited on the substrate surface are complex and not yet well understood. Anopore membranes are produced by anodic oxidation of aluminum in acid electrolytes [16]. The surface properties and morphology of Anopore alumina could be quite different from that of pyrogenic alumina used in this study. Anopore membranes provide a confinement environment with well-defined geometry, which is very different from the random voids in our systems. Therefore, one should not make direct comparison with Anopore systems and we do not consider the conclusions drawn from studies of Anopore-LC systems as applicable to our systems. Nevertheless, the Anopore results and the above discussion with detailed rationales illustrate that the experimental results could often be in conflict with arguments based on simple LC molecules-substrate interactions.

B. In-field cooling spectra

The spectra at 26 °C of IFC samples of varying alumina densities are shown in Fig. 6. Careful examination of these spectra and comparison with the corresponding ZFC spectra shown in Fig. 2 reveal that significant alignment was achieved by IFC through the $I \rightarrow N$ phase transition for all the dispersions containing hydrophobic alumina Alu C 805. But the same IFC procedure has shown rather limited alignment effect for dispersions of hydrophilic Alu C in 5CB with $\rho_s \geq 0.15$ g/cm^3 [33]. As mentioned above, networks in alumina/LC gels formed through hydrogen bonding have the ability to rearrange or reorder itself in response to external stress. It has been suggested that the formation of an anisotropic and stable network more agreeable to field-induced alignment leads to the memory effect. Similar rearrangement could occur during an IFC process. The more robust network formed by hydrophilic alumina particularly at high dispersion density, possibly coupled with a weaker surface interaction with 5CB as described above, could render the network reordering harder to occur in Alu C/5CB samples, resulting a rather limited alignment effect as observed in IFC experiments.

A more noticeable trend regarding the IFC spectra of Alu C 805/5CB (right column of Fig. 6) is the broadening of the aligned doublet with increasing alumina density, probably reflecting a distribution in void-size-dependent S values and/or less than perfect alignments. For several high-density IFC samples, these factors lead to peak splitting and two partially overlapping doublets can be easily seen. In this respect, it is of interest to examine the three 90°-orientation spectra of the same system shown in the left column of Fig. 7. They look similar to the corresponding ZFC spectra (right column of Fig. 7), except that the broad component in the 90°-orientation spectra displays much weaker shoulders and a lower but nonzero middle valley. These features clearly indicate the presence of significant but not perfect alignments in the IFC samples. The two small narrow peaks at the edge of the spectra are generated from domains that can be aligned by external magnetic field alone. Their relative intensity and position remain more or less unchanged as compared to that of the narrow doublet in the corresponding ZFC spectrum. The splitting $\Delta\nu_{90}$ in the 90°-orientation spectra is plotted against dispersion density in Fig. 8. Also included in Fig. 8 are the $\Delta\nu_p$ values from ZFC spectra of the same samples. Within experimental errors, the two set of values $\Delta\nu_{90}$ and $\Delta\nu_p$ are equal to each other. With an additional assumption that the less than perfect alignment does not affect the splitting $\Delta\nu_{90}$, the values of the two splittings can be directly related to the average order parameters S through Eq. (1) with $\theta = \pi/2$. The results indicate that the central

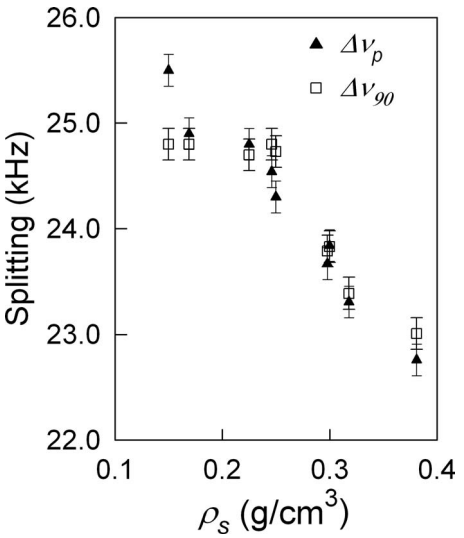

FIG. 8. The dependence on alumina density of splittings $\Delta\nu_p$ and $\Delta\nu_{90}$ of Alu C 805/5CB dispersions at 10 °C below T_{IN}. $\Delta\nu_p$ is the splitting of the Pake powder pattern in spectra of ZFC samples and $\Delta\nu_{90}$ is the splitting in spectra of IFC samples placed at 90° orientation with respect to the field direction.

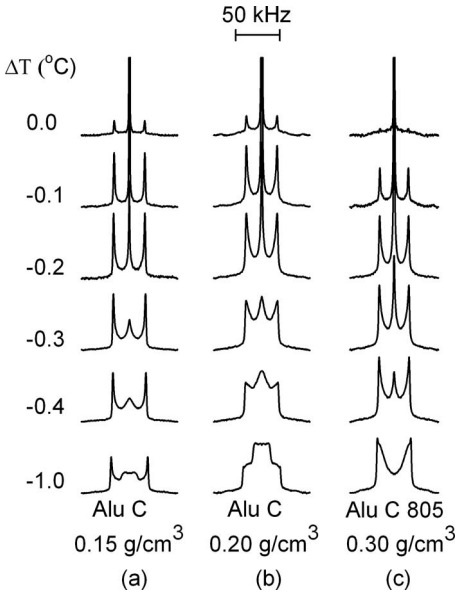

FIG. 9. Spectra recorded when slowly cooling through the $I \rightarrow N$ phase transition region. $\Delta T = T - T_{IN}$, where T_{IN} is the temperature of first appearance of the nematic phase; (a) Alu C/5CB $\rho_s = 0.15$ g/cm^3, (b) Alu C/5CB $\rho_s = 0.20$ g/cm^3, and (c) Alu C 805/5CB $\rho_s = 0.30$ g/cm^3.

broad components in corresponding ZFC and 90°-orientation IFC spectra have almost identical S values. Thus, the substantial realignment of the domain directors is brought about without discernible changes in some important characteristics of the system, i.e., there are no increases in the average order parameter of the broad component and in the percentage of domains alignable by the field effect alone. If one deems the diminution in S values as reflecting the strength of the disorder field, the results suggest that, in the aligned state produced by IFC, the disorder strength remains largely unchanged. With regard to DNMR and ESR studies of aerosil/nCB systems, we note that orientation parameters of ZFC samples have not been reported [10,11] but discussed with the suggestion that LC's in an anisotropic network (IFC samples) are expected to have a greater orientation parameter than in a random network (ZFC samples) [10]. On the other hand, it is of interest to note the recent calorimetric and x-ray scattering studies of aligned 8CB-aerosil (hydrophilic-type 300) gels prepared by thermally cycling samples numerous times through the $I \rightarrow N$ phase transition in the presence of a 2 T magnetic field [34,20]. Their somewhat unexpected results have been interpreted as indicating that the alignment of nematic domains only occurs at length scales greater than 0.2 μm, while the local gel structure at smaller length scales remains unchanged. It was further argued that the aligned aerosil gel could be stiffer than the random gel and so could impose a greater local disorder. In comparison, our results concern 5CB-alumina (hydrophobic) gels and could be interpreted as suggesting an unchanged local disorder.

Alumina gels and networks are also present in the isotropic phase. It is well known that solid surfaces exert a localized ordering effect on LC above the $N \rightarrow I$ transition temperature. The local orientational order parameter is the largest for the first surface layer of the LC molecules and it decays exponentially with increasing distance from the solid surface. The decay constant known as the nematic correlation length increases with decreasing temperature and typically measures few nm at temperatures few degrees above T_{IN}. Thus, above T_{IN} and in voids of few hundred nanometers in size, most LC molecules behave just as those in the bulk isotropic phase. During IFC through the $I \rightarrow N$ phase transition, these molecules could form well-aligned or unaligned domains depending mainly on the local disorder density or void size. To follow the development of nematic domains and their orientational profiles during IFC, we have carefully recorded the spectra in steps of 0.1 °C [35] and examined their variation through the two-phase coexistence region. Shown in Fig. 9 are three sets of spectra for three alumina/5CB dispersions of different densities, two containing Alu C and one Alu C 805. Marked on the left side of the spectra is the temperature difference $\Delta T = T - T_{IN}$, where T_{IN} is the temperature of the first appearance of nematic in each sample. All the spectra of each sample are plotted on the same intensity scale so that peak intensities at different temperatures can be compared directly.

In association with a wide distribution of void sizes, there would be a variation in transition temperatures. It is reasonable to assume LC in larger voids having a higher T_{IN} [8]. As temperature is being lowered into the two-phase coexistence region, the transition to nematic is expected to proceed first in the largest voids resulting a narrow doublet since domains in these voids could be easily and uniformly aligned by the magnetic field. With a further decrease in temperature and with the formation of more disordered nematic in smaller voids, a broad central signal could emerge. The spectra of the two Alu C/5CB samples, Figs. 9(a) and 9(b) for $\rho_s = 0.15$ and 0.20 g/cm^3, respectively, clearly testify to the sequence of the events as described. However, the intensity of the narrow doublet exhibits an unexpected temperature-dependent behavior. Their peak intensity first increases then, after reach-

ing a maximum, decreases with decreasing temperature. The maximum occurs at ΔT value of −0.2 °C and −0.1 °C in Figs. 9(a) and 9(b), respectively. Since more nematic phase is formed at lower temperature, the intensity reduction could only be attributed to an increase in the disorder strength experienced by the pertinent domains. In other words, some domains that were perfectly aligned at higher temperatures become less aligned under the influence of strengthened disorder. In relation to this interpretation, it could be of interest to mention the observed doubling of the specific-heat C_p peak in the isotropic-nematic coexistence region for several LC-aerosil dispersions [36,37]. The two-step $I \rightarrow N$ transition has been ascribed to variations in coupling strength with the embedded solid network in the two-phase coexistence region. It has been speculated that just below the T_{IN}, the LC molecules are shielded from the surface effects by a paranematic layer covering the aerosil strands and, thus, are free to form uniformly aligned nematic domains. The thinning of the paranematic layer at lower temperature re-establishes the strong coupling and effectively increases the disorder strength experienced by the void nematics. Our DNMR results can be interpreted as clear evidence for the growth of disorder strength through the $I \rightarrow N$ transition. In comparison, the spectra of sample Alu C 805/5CB of $\rho_s = 0.30$ g/cm^3 [Fig. 9(c)] were altered by the presence of IFC effected alignment. The formation of nematics in smaller voids leads to a broadening of the narrow doublet instead of generating a central broad signal. Thus, "field-aid" annealing processes mask the effects of augmented disorder strength experienced by the domains, and the doublet intensity remains more or less constant through the two-phase coexistence region. In the above discussion, the variation in spectral features has been related to the interpretation proposed for the observed doubling of specific-heat peak during the $I \rightarrow N$ phase transition in several aerosil/LC dispersions. It should be pointed out that we are not aware of any experimental studies of alumina-LC systems using techniques, such as high-resolution calorimetry, which are capable of detecting the presence of double C_p peaks in the two-phase coexistence region.

To investigate the stability of the alignment generated with IFC, DNMR spectra of IFC samples were measured again days or weeks after the initial experiments. Samples were stored at 30 °C in an incubator between measurements. Examples of these measurements shown in Fig. 10 evidence the "memory effect." Even for a sample showing a significant deterioration of alignment with time, such as Alu C 805/5CB of $\rho_s = 0.30$ g/m^3 [Fig. 10(b)], the system did not return to the original "random" state but approached a state with considerable remnant order.

IV. CONCLUSIONS

This work presents a DNMR study of dispersions prepared by ZFC and IFC procedures of hydrophilic and hydrophobic pyrogenic alumina in liquid-crystal 5CB. The disorder effects of embedded alumina matrix on void nematics were examined as functions of temperature and alumina density ρ_s. The spectra of most ZFC samples showing a narrow doublet with a broad central Pake pattern indicate there is a wide distribution of void sizes. At a given $(T - T_{IN})$, the average orientational order parameter (S_p) of the observed broad Pake pattern decreases with increasing alumina density, reflecting an elevation of the strength of the random field. The order parameters and their variation with ρ_s also suggest a stronger disordering effect from the nonpolar surface of Alu C 805 particles.

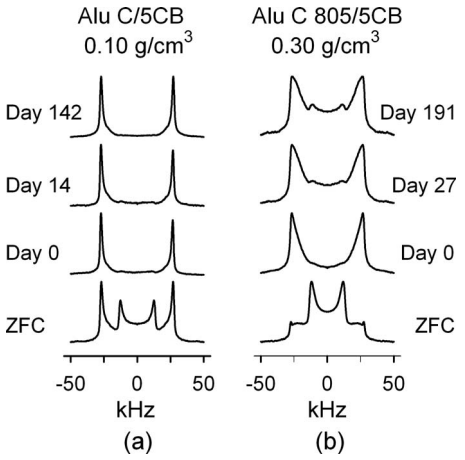

FIG. 10. Spectra at 26 °C of two IFC samples recorded on different days after the initial IFC experiment; (a) Alu C/5CB $\rho_s = 0.10$ g/cm^3 and (b) Alu C 805/5CB $\rho_s = 0.30$ g/cm^3. For comparison, the original ZFC spectra are also included.

Significant alignment was achieved by IFC through the $I \rightarrow N$ phase transition for all the dispersions containing hydrophobic alumina Alu C 805, while very limited alignment effects were found for dispersions of hydrophilic Alu C in 5CB with $\rho_s \geq 0.15$ g/cm^3. The difference is attributed to the stronger network formed by hydrophilic alumina coupled with weaker interactions of 5CB with the surface of the dispersed Alu C particles. To further characterize the aligned Alu C 805/5CB gels, the IFC spectra and their angle dependence are carefully examined and are compared with the corresponding ZFC spectra. The results indicate that within the experimental error, the imposition of substantial alignment alters neither the average order parameter of affected domains nor the percentage of domains alignable by the field effect alone. In addition, sequences of spectra of several selected dispersions are presented to detail the variation in spectra features within the nematic-isotropic coexistence region and to illustrate the effect of increasing disorder strength during the phase transition.

On the whole, the alumina/5CB dispersions show behaviors comparable to those of aerosil/nCB dispersions with similar void sizes. However, differences have been noticed in IFC experiments, probably due to the basic character of surface hydroxyl groups of hydrophilic alumina, which weakens the interactions with 5CB molecules. Another possible difference could be the relative strength of disordering effects of hydrophilic vs hydrophobic particles.

ACKNOWLEDGMENTS

Financial support from the Quebec Government (Fonds

Québécois de la Recherche sur la Nature et les Technologies) is gratefully acknowledged. We thank Dr. Frederick Morin of the McGill NMR facility for his assistance, and Dr. Gerald Brydon of Dawson College for helpful discussions. We would like to thank Professor Linda Reven and members of her research group at McGill University for many stimulating discussions.

[1] *Liquid Crystals in Complex Geometries Formed by Polymer and Porous Networks*, edited by G. P. Crawford and S. Žumer (Taylor & Francis, London, 1996).
[2] R. Eidenschink and W. H. De Jeu, Electron. Lett. **27**, 1195 (1991).
[3] M. Kreuzer, T. Tschudi, and R. Eidenschink, Mol. Cryst. Liq. Cryst. **223**, 219 (1992).
[4] M. Kreuzer and R. Eidenschink, in *Liquid Crystals in Complex Geometries Formed by Polymer and Porous Networks* (Ref. [1]), Chap. 15, p. 307.
[5] D. Sikharulidze, Appl. Phys. Lett. **86**, 033507 (2005); C. Huang, C. Lai, Y. Tseng, Y. Yang, C. Tien, and K. Lo, *ibid.* **92**, 221908 (2008).
[6] T. Bellini, M. Buscaglia, C. Chiccoli, F. Mantegazza, P. Pasini, and C. Zannoni, Phys. Rev. Lett. **85**, 1008 (2000); M. Rotunno, M. Buscaglia, C. Chiccoli, F. Mantegazza, P. Pasini, T. Bellini, and C. Zannoni, *ibid.* **94**, 097802 (2005); M. Buscaglia, T. Bellini, C. Chiccoli, F. Mantegazza, P. Pasini, M. Rotunno, and C. Zannoni, Phys. Rev. E **74**, 011706 (2006).
[7] One of the referees has suggested the following experiment to distinguish the two possible sources for an observed memory effect. The *aligned* sample is temperature cycled through the isotropic phase outside the field. If the nematic alignment persists then one can conclude that gel restructuring has occurred [20].
[8] G. S. Iannacchione, C. W. Garland, J. T. Mang, and T. P. Rieker, Phys. Rev. E **58**, 5966 (1998).
[9] G. S. Iannacchione, Fluid Phase Equilib. **222-223**, 177 (2004).
[10] T. Jin and D. Finotello, Phys. Rev. E **69**, 041704 (2004).
[11] A. Arcioni, C. Bacchiocchi, L. Grossi, A. Nicolini, and C. Zannoni, J. Phys. Chem. B **106**, 9245 (2002); A. Arcioni, C. Bacchiocchi, V. G. Vecchi, and C. Zannoni, Chem. Phys. Lett. **396**, 433 (2004).
[12] J. Milette, C. T. Yim, and L. Reven, J. Phys. Chem. B **112**, 3322 (2008).
[13] Technical Bulletin Pigments, Number 56, Highly Dispersed Metallic Oxides Produced by the AEROSIL® Process, Degussa Cooperation; A. Bogdan and M. Kulmala, in *Encyclopedia of Surface and Colloid Science*, edited by P. Somasundaran, 2nd ed. (Taylor & Francis, New York, 2006), p. 5314.
[14] M. Vilfan, B. Zalar, G. P. Crawford, D. Finotello, and S. Žumer, in *Surfaces and Interfaces of Liquid Crystals*, edited by T. Rasing and I. Muševič (Springer-Verlag, Berlin, 2004), Chap. 2, p. 17.
[15] G. P. Crawford, R. J. Ondris-Crawford, J. W. Doane, and S. Žumer, Phys. Rev. E **53**, 3647 (1996).
[16] R. E. Benfield, D. Grandjean, J. C. Dore, H. Esfahanian, Z. Wu, M. Kröll, M. Geerkens, and G. Schmid, Faraday Discuss. **125**, 327 (2004).
[17] G. W. Gray and A. Mosley, Mol. Cryst. Liq. Cryst. **48**, 233 (1978); **35**, 71 (1976).
[18] H. Haga and C. W. Garland, Phys. Rev. E **56**, 3044 (1997).
[19] L. Wu, B. Zhou, C. W. Garland, T. Bellini, and D. W. Schaefer, Phys. Rev. E **51**, 2157 (1995); H. Zeng, B. Zalar, G. S. Iannacchione, and D. Finotello, *ibid.* **60**, 5607 (1999).
[20] D. Liang, M. A. Borthwick, and R. L. Leheny, J. Phys.: Condens. Matter **16**, S1989 (2004).
[21] D. Sharma, J. C. MacDonald, and G. S. Iannacchione, J. Phys. Chem. B **110**, 26160 (2006).
[22] P. G. de Gennes and I. Prost, *The Physics of Liquid Crystals* (Oxford University Press, Oxford, 1993).
[23] E7 is a commercial LC mixture containing 51% 4′-n-pentyl-4-cyanobiphenyl, 25% 4′-n-heptyl-4-cyanobiphenyl, 16% 4′-n-octoxy-4-cyanobiphenyl and 8% 4″-n-pentyl-4-cyano-p-terphenyl.
[24] A. Golemme, S. Žumer, J. W. Doane, and M. E. Neubert, Phys. Rev. A **37**, 559 (1988).
[25] D. A. Dunmur, in *Physical Properties of Liquid Crystals: Nematic*, edited by D. Dunmur, A. Fukuda, and G. Luckhurst (Inspec, London, 2001), Sec. 5.2, p. 216.
[26] J. D. Bunning, D. A. Crellin, and T. E. Faber, Liq. Cryst. **1**, 37 (1986).
[27] W. Haase, in *Physical Properties of Liquid Crystals: Nematic* (Ref. [25]), Sec. 6.3, p. 288.
[28] All quantities in Eq. (2) should be in SI units. The $\Delta\chi$ values, given in CGS units in Ref. [26], have been multiplied by 4π to convert them to values in SI units.
[29] For all the dispersions studied, the observed T_{IN} is lower than that of the pure 5CB. Their values scatter about 0.4 °C below the T_{IN} of 5CB and within ranges of ±0.2 °C and ±0.3 °C for Alu C/5CB and Alu C 805/5CB, respectively. The more or less constant T_{IN} values could be considered as indicating the presence of a shallow T_{IN} minimum, which has been reported for aerosil/8CB dispersions with comparable void sizes. However, in view of the uncertainty in the measured T_{IN} value (±0.20 °C), we are reluctant to speculate relationships between ΔT_{IN} and ρ_s values. We attribute the observed small variation of T_{IN} with ρ_s to the limited range of void sizes covered in this study.
[30] G. A. Jeffrey, *An Introduction to Hydrogen Bonding* (Oxford University Press, New York, 1997).
[31] B. Jerome, Rep. Prog. Phys. **54**, 391 (1991).
[32] B. Zalar, R. Blinc, S. Žumer, T. Jin, and D. Finotello, Phys. Rev. E **65**, 041703 (2002).
[33] As suggested by the strong temperature dependence of ZFC spectra of Alu C/5CB ρ_s=0.10 g/cm^3, shown in Fig. 3 left column, almost all domains will become aligned when the sample temperature reaches the T_{IN} (36 °C), i.e., before performing the IFC procedure. Thus, the well-aligned IFC spectrum of the same sample (Fig. 6, left column, second spectrum from the bottom) cannot be taken as evidence that IFC procedure is more effective in producing aligned states at ρ_s =0.10 g/cm^3.

[34] F. Crucenau, D. Liang, R. L. Leheny, and G. S. Iannacchione, Liq. Cryst. **35**, 1061 (2008).

[35] Spectra were monitored after an initial waiting period of ~10 min to verify that the two-phase system had reached thermal equilibrium at the selected temperature as indicated by the identical spectra being observed in successive recordings.

[36] M. Caggioni, A. Roshi, S. Barjami, F. Mantegazza, G. S. Iannacchione, and T. Bellini, Phys. Rev. Lett. **93**, 127801 (2004); F. Mercuri, S. Paoloni, U. Zammit, and M. Marinelli, *ibid.* **94**, 247801 (2005).

[37] A. Roshi, G. S. Iannacchione, P. S. Clegg, and R. J. Birgeneau, Phys. Rev. E **69**, 031703 (2004).